J. Chem. Soc., Faraday Trans. 2, 1987, **83**, 1189–1203

Electronic Structure and Ground-state Properties of the Actinide Dioxides

Paul J. Kelly
Philips Research Laboratories, 5600 JA Eindhoven, The Netherlands

M. S. S. Brooks
European Institute for Transuranium Elements, 7500 Karlsruhe, Federal Republic of Germany

We use the linear muffin-tin orbital method and the local density approximation to calculate the cohesive energies, equilibrium lattice constants and bulk moduli of ThO_2, UO_2 and PuO_2. These calculations provide a framework within which to discuss the bonding in this system. The band structure of UO_2 is examined in particular detail and its volume dependence is discussed.

In this paper we consider the electronic structure of the actinide dioxides ThO_2, UO_2 and PuO_2. While the oxides of most technological importance are rarely stoichiometric, we choose to study the fluorite structured oxides AnO_2 (An = actinide) because they form a system which is relatively simple to characterize experimentally and study in detail both theoretically and experimentally.

A simple picture of the electronic structure of fluorite-structured AnO_2 is as follows. We first consider the oxygen sublattice, which is simple cubic, and form AnO_2 by inserting an An atom at the body centre of every other cube. The simple cubic oxygen sublattice gives rise to a single band originating from the atomic 2*s* state, which is separated by *ca.* 14 eV from the band formed from the 2*p* states. The next oxygen-derived band is a broad band formed from the unoccupied 3*s* states. Inserting an An atom doubles the size of the unit cell in real space and leads to a folding of the oxygen bands into bonding and antibonding states and splitting of the bands at the zone boundary. At the centre of the Brillouin zone the 2*s* and 3*s* states transform as Γ_1 and Γ_2', while the 2*p* states transform as a bonding Γ_{25}' state and an antibonding Γ_{15} state. This is not, of course, the only effect of introducing the An atom. Its atomic states also give rise to bands. Below the oxygen 2*s* bands the filled An 6*p* states form a band (with large spin–orbit splitting), the 6*d* states give rise to a conduction band *ca.* 5–6 eV above the top of the oxygen 2*p* band, and in this so-called fundamental gap fall the localized An 5*f* states. Charge transfer from An to oxygen leads to a filling of the oxygen 2*p*-derived band and hence a nominal 4+ oxidation state of the An ion. In this simple picture there are no occupied thorium *f*-like states in ThO_2, and additional electrons added as we go across the actinide series are assumed to go into *f*-like states. Thus there are two filled uranium *f*-like states in UO_2 and four filled plutonium *f*-like states in PuO_2.

Thorium dioxide forms stoichiometrically and is a wide-gap transparent insulator. The optical gap determined from measurements of the absorption threshold on thin films of ThO_2 is *ca.* 6 eV.[1] X.p.s. measurements[2,3] indicate a valence bandwidth of *ca.* 5 eV and no state density at E_F.

UO_2 is a coloured semiconductor which tends to form hyperstoichiometrically. It orders antiferromagnetically below 30 K. Form factor measurements[4,5] indicate that the magnetism is due to two unpaired *f* electrons. Early optical absorption measurements[6]

indicated one absorption band between 2.5 and 5.2 eV with a maximum at *ca.* 3.9 eV and a second strong absorption band starting at *ca.* 5.2 eV. However, the transitions involved were not identified. From optical reflectivity and absorption measurements over a larger spectral range, Schoenes[7] confirmed the earlier measurements and identified the first absorption band as being due to $f^2 \rightarrow f^1 d$ transitions. The second 'fundamental' absorption band arises from O $2p$ to U d transitions. A coherent picture of the electronic structure of UO_2 has finally emerged from photoelectron spectroscopy studies.[2,3,8–12] X-Ray (X.p.s.) and ultraviolet (U.p.s.) photoelectron spectroscopy have been used to probe the occupied states and bremsstrahlung isochromat spectroscopy (b.i.s.) to probe the unoccupied states. The electronic structure from this work is in agreement with that derived from optical reflectivity and absorption.[7] The experimental situation is reviewed by Schoenes in ref. (13) and also in this volume.

For PuO_2, only X.p.s. measurements have been reported.[14,15] The $5f$ states lie lower than in UO_2 and appear to overlap the $2p$ valence band, which together appear to have a width of *ca.* 5 eV.

There have been few calculations of the electronic structure of the actinide dioxides. Gubanov *et al.*[16] have performed non-self-consistent molecular cluster calculations within the local density (LD) approximation for clusters simulating rocksalt- and fluorite-structured (sixfold and eightfold coordinated, respectively) thorium and uranium oxides. Relativistic and spin-polarization effects were studied. Relativistic extended Hückel molecular cluster calculations were performed by Courteix *et al.*[15] to help interpret their X.p.s. spectra for PuO_2.

Exploratory band-structure calculations by Kelly *et al.*[17] demonstrated the necessity to make such calculations self-consistent. The results of subsequent self-consistent LD calculations gave good agreement for the ground-state properties of UO_2 so long as the f states were not treated as pure band states.[18,19] In the following section we state briefly the basis of density functional (DF) theory and discuss its limitations and those of the local density approximation which has been used in almost all DF calculations to date.[20] We then present the results of the calculations of the cohesive properties of ThO_2, UO_2 and PuO_2 and go on to discuss the corresponding electronic structures.

Method of Calculation

In density-functional theory[20–22] the ground-state energy of an interacting inhomogeneous electron system in an external potential may be obtained by solving a simple single-particle-like Schrödinger equation where the effects of exchange and correlation are included in a local exchange-correlation potential. The eigenvalues which occur in this Schrödinger equation serve as auxiliary quantities to calculate the total energy. A physical meaning has been given to only the last occupied eigenvalue, which has been shown to be equal to the ionization potential.[23] Otherwise the eigenvalues should not be identified with excitation energies although, in the absence of any other first principles calculations, this is frequently done. Exact DF calculations for light atoms indicate that the eigenvalues interpreted as excitation energies underestimate these energies.[24]

While the density-functional formalism is exact and can, in principle, describe strongly correlated localized states as well as itinerant states, in practice some approximation has to be made for the exchange-correlation energy functional and potential. In almost all cases that approximation is the so-called local density (LD) approximation, where the exchange-correlation energy of the inhomogeneous system is expressed in terms of the exchange-correlation energy of a homogeneous interacting electron gas calculated for different densities. Many calculations of ground-state properties have been carried out with the LD approximation with a great deal more success than might be expected from simple considerations of its realm of validity.[25]

Where the exact DF eigenvalues do not in general yield excitation energies the LD eigenvalues are, *a fortiori*, to be trusted even less.[24] They may be used for qualitative purposes which depend only on the symmetry and relative positioning of the energy bands. A quantitative discussion of excitation energies requires a calculation of the electron self-energy, for which the LD approximation is a convenient starting point. Such calculations have been carried out for the first time only recently for silicon and diamond.[26] They yield results in excellent agreement with experiment even though the LD eigenvalues, in these cases, seriously underestimate the band gap.

Our discussion of the electronic structure of the actinide dioxides will therefore be mainly concerned with the calculation of the ground-state properties, and comparison with experiments which measure excitation energies will only be made in passing.

The method[27] we use to solve the Schrödinger equation is the linear muffin-tin orbital (LMTO) method, together with the so-called atomic-sphere approximation (ASA). In the ASA the polygonal Wigner-Seitz cells are replaced by spheres of the same volume. This method, combined with the LD approximation, has been applied to many systems and shown to be a very efficient means of solving the Schrödinger equation with only a small loss of accuracy.[28] Even systems with low coordination number can be treated within the ASA by the introduction of so-called empty spheres. These are additional scattering centres introduced into the lattice to increase the variational flexibility in the description of the electron charge density. This has been demonstrated to work very well for the diamond and zinc blende lattices,[29,30] where the results obtained are essentially indistinguishable from those obtained by methods without any restriction on the form of the potential. For the fluorite lattice we include an empty sphere on the body-centred site of the oxygen sublattice which does not contain an An atom.

For heavy elements it is necessary to take into account relativistic effects.[31] Since the states which are responsible for bonding in AnO_2 are either completely filled or have a small spin-orbit splitting we use a so-called semi-relativistic approximation, which includes the mass-velocity and Darwin shifts but leaves out spin-orbit coupling with substantial computational saving.[32]

Ground-state Properties

In order to describe the ground-state properties of the light actinide metals or the metallic NaCl structured chalcogenides or pnictides, an itinerant description of the *f* electrons is necessary and the LD approximation appears to work quite well.[31] By carrying out band-structure calculations for ThO_2 and UO_2 with the *f* electrons in band states we will see that the LD approximation, as might be expected in this case, fails to describe the ground-state properties correctly. It predicts lattice constants that are too small and overestimates the binding. Treatment of the *f* states as purely atomic-like states results in good values for the lattice constants, bulk moduli and cohesive energy. By populating the *f* bonding and antibonding states equally, hybridization with the oxygen valence states can be taken into account without affecting the ground-state properties appreciably.

ThO_2

Fig. 1 shows the total energy[33] as a function of the lattice constant minus the atom energies for ThO_2. The upper curve was calculated by omitting *f* states totally from the calculation. The lower curve was calculated by treating the *f* states as normal band states. The crosses are calculated values from which the equilibrium lattice constant, the bulk modulus and the cohesive energy are obtained by a least-squares fit to a cubic polynomial in the volume. These are given in table 1 for the upper curve together with the experimental values. Clearly, these calculated results are in satisfactory agreement

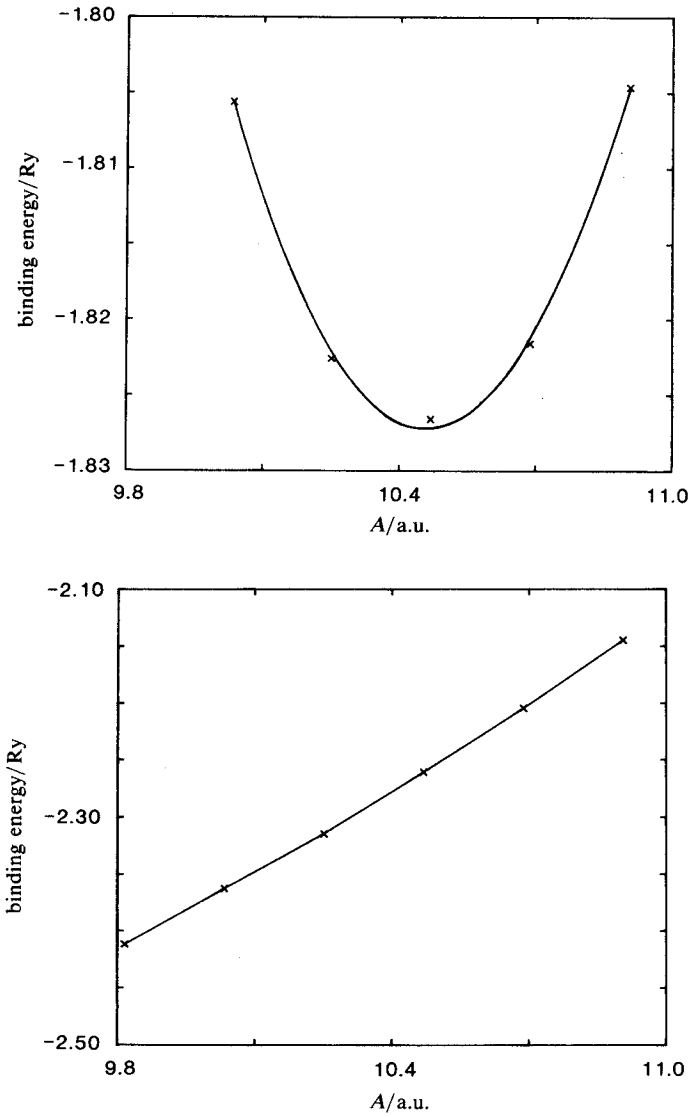

Fig. 1. Total energy *vs.* lattice constant for ThO_2. The crosses represent calculated values and the upper solid curve is the least-squares fitted cubic polynomial in the volume. In the upper curve no f electrons were included and in the lower curve the f states were included in the calculation as ordinary band states. The atom energies have been subtracted so that the minimum in the upper curve is the cohesive energy given in table 1.

Table 1. Comparison of experimental and calculated values of the lattice constant A, the bulk modulus B and the cohesive energy E_c of ThO_2

	A/a.u.	B/Mbar	E_c/Ry
calcd	10.46	2.9	1.83
exptl	10.576	2.78	1.74

with experiment. The binding energy curve can be analysed in more detail using the so-called pressure formula.[34] This has been done for UO_2 and CaF_2 in ref. (18). The basic result is that the binding energy is indeed predominantly ionic in nature, but there is also a substantial cation d bonding interaction (covalency). Use of the pressure formula gives more insight into the microscopic details of the repulsive interaction which in the ionic model is purely phenomenological.

From fig. 1 it is clear that inclusion of the f states as band states leads to an unphysical collapse of the lattice. At a volume 20% below the experimental equilibrium volume the binding energy is still decreasing with little sign of a minimum. Even though ThO_2 is normally considered to have no f electrons the inclusion of the $5f$ states leads to quite a broad band at the top of the fundamental gap and this band hybridizes strongly with the oxygen p states. The extent of this hybridization is shown in fig. 2, where the total density of states (DOS), as well as the thorium projected DOS, the oxygen projected DOS and thorium f DOS, are plotted at the experimental equilibrium lattice constant. By integrating the partial DOS, $N_{tl}(E)$, up to the Fermi energy one obtains n_{tl}, the number of electrons with angular momentum l and atomic character t. The thorium ionicity which is obtained by integrating the charge inside the thorium atomic sphere is plotted as a function of volume in fig. 3 for the cases where f states are included and not included. For the former case the number of thorium f-like electrons is seen to be *ca.* 1. In both cases there is a large deviation from the nominal full (4+) ionicity. Since the definition of ionicity used above is largely arbitrary, depending as it does on how one chooses to divide up space with the space-filling spheres used in the ASA, it is worthwhile digressing for a moment on the choice used in the calculations presented here.

There are two basic considerations in the choice of sphere sizes. One is that the overlap of atomic spheres on neighbouring sites should be as small as possible. For the b.c.c lattice, to which the fluorite lattice reduces when all lattice sites (including the 'empty' site) are the same, this overlap is 13.7%. The second consideration is that the spheres should contain the atomic cores. The actinide $6s$ and $6p$ core states are very extended and dictate a large cation atomic sphere. The effect of changing the relative sphere sizes is seen in fig. 4. Here the total energy of ThO_2 (omitting the thorium f states) is plotted as a function of the thorium atomic sphere radius for a fixed volume equal to the calculated equilibrium volume. Around a thorium sphere radius of 2.8 a.u. the total energy is only weakly dependent on the choice of sphere sizes. This sphere size of 2.8 a.u. corresponds to an overlap of thorium and oxygen atomic spheres of 16.8%. If possible, calculations should be carried out in this region. In order to achieve this division of space it was necessary to include the thorium $6p$ and oxygen $2s$ states explicitly as band states. Also shown in fig. 4 is the net charge on the thorium atomic sphere as that sphere radius is changed. It changes almost linearly over the range where the energy is roughly constant. To obtain a 4+ thorium atom the thorium sphere size must be reduced to <2.6 a.u. However, for a sphere radius <2.7 a.u. the $6s$ states must be included explicitly as band states in the calculation, otherwise they must be renormalized quite substantially. Thus the resulting 4+ ion has been obtained by excluding cation $6s$ and $6p$ core charge density from the cation sphere and is therefore quite different from the classical 4+ thorium ion, which retains an integral core. That it is so difficult to obtain a 4+ thorium atom is not surprising. In a quantum-mechanical calculation the mechanism providing the repulsive interaction, the so-called core repulsion, arises from the interaction between the valence and core states when they overlap spatially. This interaction gives charge in the nominal anion valence bands cation-like character.

In the calculations in fig. 1 a larger cation sphere size than the ideal value was used in order to be able to decrease the volume without renormalizing too much of the thorium $6s$ charge density. From fig. 4 we can estimate that the theoretical value for the cohesive energy in table 1 should be 80 mRy larger or 1.91 Ry, which is still in very

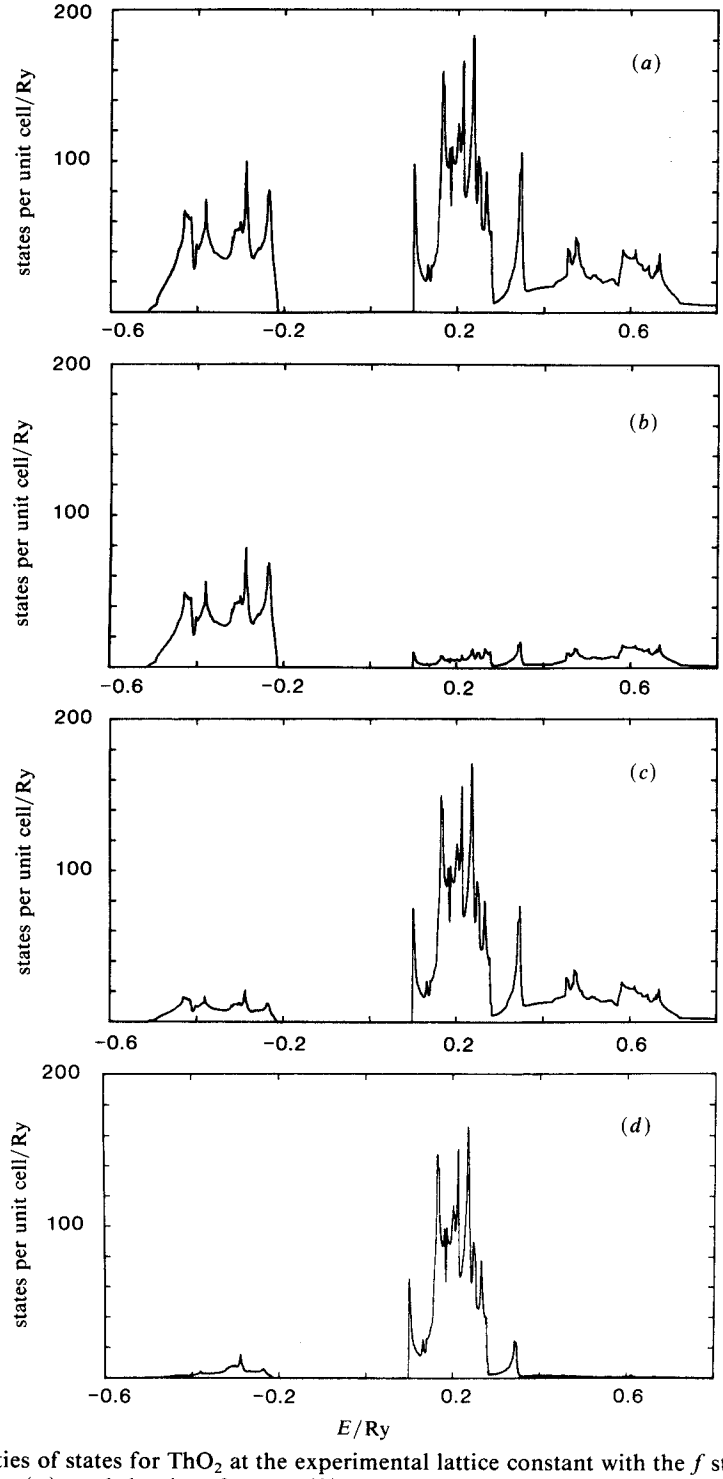

Fig. 2. Densities of states for ThO_2 at the experimental lattice constant with the f states included as band states: (*a*) total density of states, (*b*) total oxygen projected density of states, (*c*) total thorium projected density of states and (*d*) thorium f projected density of states.

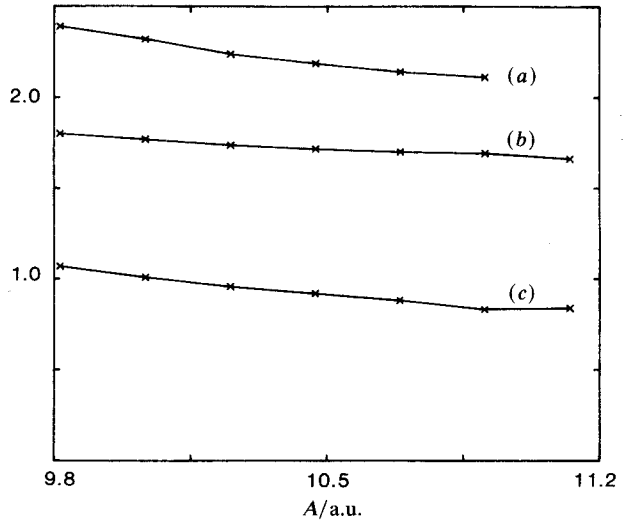

Fig. 3. Total charge on a thorium sphere in ThO_2 as a function of the lattice constant. (*a*) no *f* electrons included, (*b*) with *f* electrons included as band electrons and (*c*) total number of *f* electrons when included as band states.

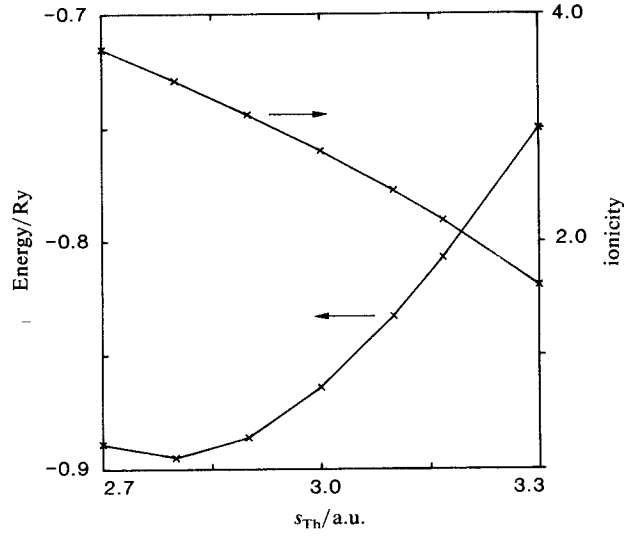

Fig. 4. Total energy of ThO_2 (to within an arbitrary constant) and total charge on a thorium sphere as a function of the thorium Wigner-Seitz sphere radius s_{Th} at the experimental lattice constant. No *f* states were included.

good agreement with experiment. This corrected value is given later in table 3, together with the corresponding calculated and measured values for UO_2 and PuO_2.

UO_2

The inclusion of the uranium *f* states as ordinary band states leads to a lattice collapse as already found above for ThO_2. These results are given in row (i) of table 2. The

Table 2. Comparison of experimental and calculated values of the lattice constant, A, the bulk modulus, B and the cohesive energy E_c of UO_2 for different treatments of the f electrons [a]

	A/a.u.	B/Mbar	E_c/Ry
(i)	<8.9	—	>2.7
(ii)	10.14	—	1.64
(iii)	10.01	2.3	1.70
(iv)	10.336	2.09	1.64

[a] In row (i) the f electrons are included as ordinary band electrons while in row (ii) they are treated as atomic-like states but recalculated every iteration in the new potential. In row (iii) they are again included as band electrons but each f band is filled with 1/7th of an electron. The experimental values are given in row (iv).

equilibrium lattice constant was not found in this case but is at least 10% (or 30% in volume) too small and the cohesive energy grossly overestimated. Treating the f states as atomic-like states but recalculated in the self-consistent potential results in reasonable values for the lattice constant and cohesive energy [row (ii) of table 2]. When this is done, the amplitude of the $5f$ orbital at the sphere boundary is sufficiently large that substantial hybridization with the oxygen p states might be expected. The treatment adopted in ref. (19) allows this hybridization to take place without the lattice collapsing. The f states were treated as band states, but in order to achieve a filled (non-conducting and non-bonding) band only 1/7th of an electron was placed in each f state. Thus the f bands are filled with a total of two electrons. This results in a lattice constant which is *ca.* 3% too small, a cohesive energy which is *ca.* 10% too large and a bulk modulus quite close to the experimental value [rows (iii) and (iv) of table 2]. The agreement is comparable to that found for ThO_2. By comparison with row (ii) of table 2 it can be seen that the effect of allowing the $5f$ states to hybridize as above increases the cohesive energy slightly. The extent to which the $5f$ states mix into the valence band could be determined experimentally by energy-dependent or angle-resolved photoemission as will be discussed later on.

PuO_2

The calculations for PuO_2 were performed using the same device as that described above for UO_2 to achieve a filled f band. In this case 4/14th of an electron were placed in each f state so that the f bands are filled with four electrons. The energy *vs.* volume curve is shown in fig. 5 and the results summarized in table 3 together with the corresponding results for ThO_2 and UO_2. The calculated lattice constant is 2% smaller than experiment and the cohesive energy only 40 mRy smaller. The bulk modulus is not accurately known, but from the trend in the bulk moduli of ThO_2, UO_2 and NpO_2 (2.78, 2.07 and 2.00 Mbar, respectively) we expect a value of B of slightly less than 2 Mbar for PuO_2. The calculated value is close to this, but because the total energies for PuO_2 are only converged to mRy accuracy the calculated bulk modulus has an uncertainty of *ca.* 30%.

The above calculations have been performed with many approximations (LD, LMTO-ASA, frozen cores *etc.*) but no adjustable parameters. The only quantity empirically adjusted is the number of f electrons, which, however, can be inferred from experiment. Calculations carried out with the f electrons in bands give unphysical results and it is

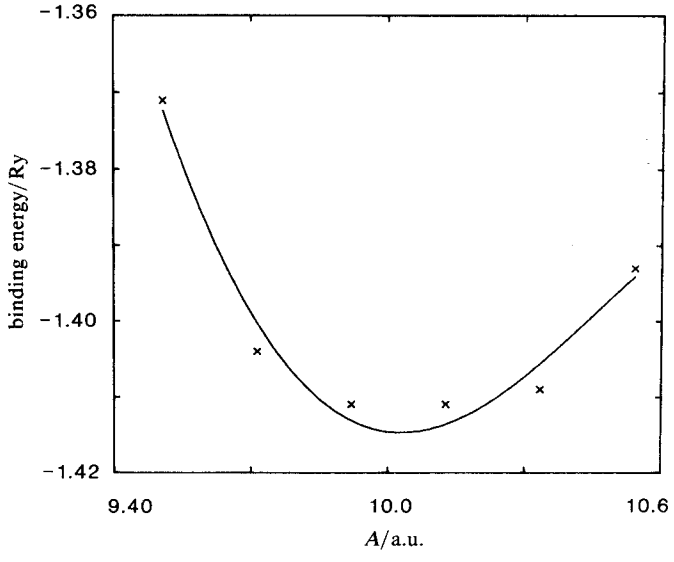

Fig. 5. Total energy *vs.* lattice constant for PuO_2. The crosses represent calculated values and the solid curve is the least-squares fitted cubic polynomial in the volume. The atom energies have been subtracted so that the minimum is the cohesive energy given in table 3.

Table 3. Comparison of experimental and final calculated values of the lattice constant, A, the bulk modulus, B and the cohesive energy E_c for ThO_2, UO_2 and PuO_2

	A/a.u.		B/Mbar		E_c/Ry	
	calcd	exptl	calcd	exptl	calcd	exptl
ThO_2	10.46	10.576	2.9	2.78	1.91	1.74
UO_2	10.01	10.336	2.3	2.07	1.70	1.64
PuO_2	10.03	10.195	1.9	—	1.41	1.45

reasonable to treat the f electrons as atomic-like. Nevertheless, this represents a weak point if one is interested in predicting the number of f electrons on the An atom. An example of this would arise if an An atom occupied a site other than its regular lattice site. With this proviso, all of the quantities calculated which can be compared directly are in reasonable agreement with experiment. The cohesive energy, E_c, is the energy gained in the ground state of the solid with respect to the component neutral free atoms. It can be determined experimentally by measuring the heat of formation, H, of AnO_2 (starting with An metal and O_2 molecules), the sublimation energy, S, of An metal and the dissociation energy, D, of O_2. Thus

$$E_c = S + D - H.$$

The values of S and H for ThO_2, UO_2 and PuO_2 needed to calculate E_c in table 3 were taken from ref. (35) and D was taken to be 376 mRy from ref. (36).

The only other attempts we are aware of to calculate the binding energy of AnO_2 use the so-called ionic model.[37,38] What is calculated in this case is a cohesive energy with, as reference, not neutral atoms but ions (An^{4+} and O^{2-}), so that the resulting lattice energy is much larger than E_c above (for UO_2, *ca.* 7.6 Ry compared to 1.7 Ry). In order to compare the lattice energy with experiment it is necessary to know the

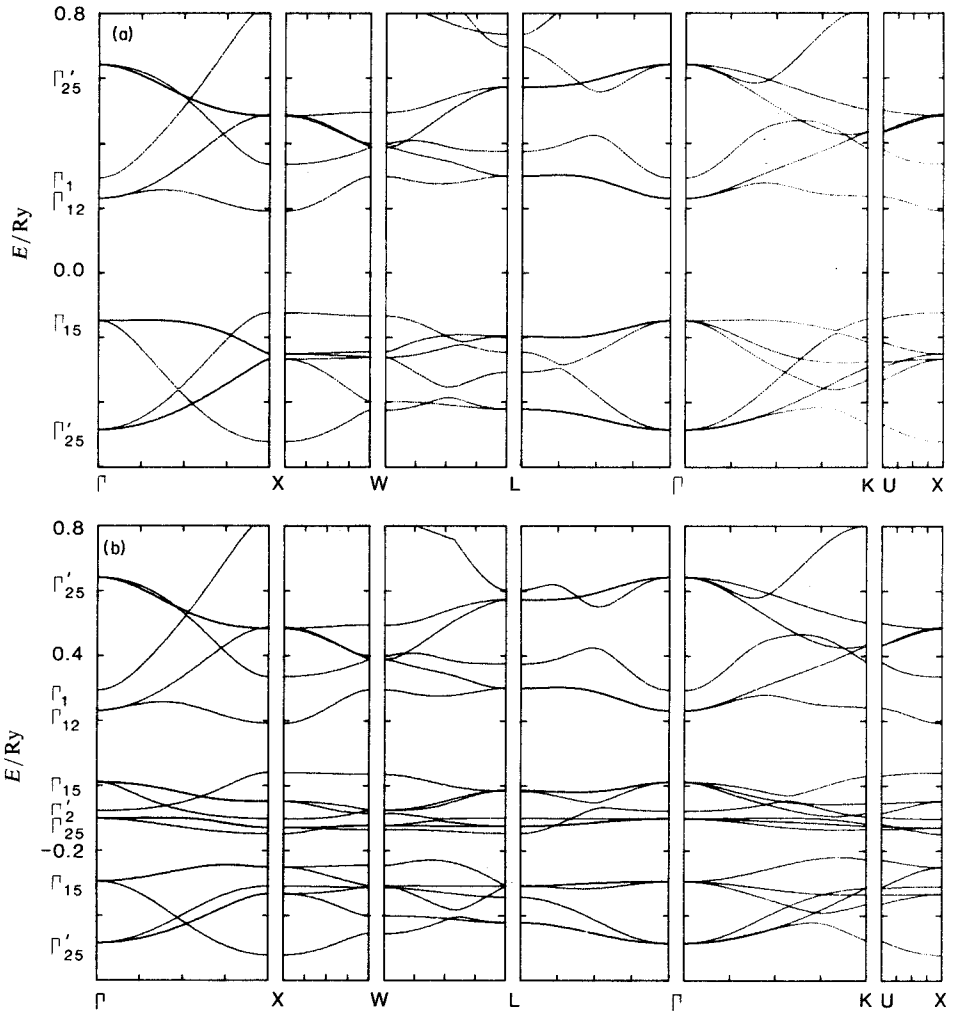

Fig. 6. Energy-band structure of UO_2 at the experimental lattice constant along some lines of high symmetry: (*a*) without and (*b*) with *f*-band states.

corresponding ionization energies and affinities. For the actinides these are not known reliably and oxygen does not bind two electrons, so that estimates of these quantities must be made. Nevertheless, the ionic model forms the basis[39] for almost all defect calculations in AnO_2. The relevance of our work to this issue is that we find that a 4+ ion in AnO_2 can only be obtained at the expense of corrupting the cation $6s^2,6p^6$ core. In cases where difficulties are encountered with the ionic model it may be necessary to take account of the covalent interaction in AnO_2.

Electronic Structure

UO_2

The band structure of UO_2 at the experimental lattice constant is shown in fig. 6 along several high-symmetry directions. In the upper panel the *f* states have been omitted. The main features of the band structure without the *f* states are, as described in the introduction, a valence band derived from the oxygen *p* states and a conduction band

derived from the uranium $6d$ and $7s$ and the oxygen $3s$ states. These bands are separated by a direct gap of 4.3 eV at the X point. The valence band is also widest at the X point (5.4 eV). The splitting of the bonding and antibonding combinations of the p states is smaller (4.6 eV) at the Γ point, where the vertical gap is 5.2 eV. The large valence bandwidth of >5 eV is a measure of the strong covalent interaction on the anion sublattice.

The conduction-band minimum at X is *ca.* 0.5 eV below the minimum at Γ. This latter minimum is formed from the doubly degenerate Γ_{12} combination of the uranium d levels, which also give rise to a Γ'_{25} level that lies 5.6 eV higher. The $6d$ band is crossed by a singly-degenerate s band with mixed uranium and oxygen character. This band lies between the crystal-field-split $6d$ levels at Γ, where it transforms as Γ_1.

In the lower panel of fig. 6 the f states are included as band states. The band which they then form is 2.5 eV wide and lies in the fundamental bandgap. In the absence of spin–orbit coupling the 7 $5f$ states transform under cubic symmetry at Γ as Γ_{25}, Γ'_2 and Γ_{15}. They interact strongly with the top of the valence band, depressing it by almost 2.0 eV. The valence bandwidth is reduced by 1.7 to 3.7 eV at X and the fundamental bandgap is increased by the same amount because the interaction of the f states with the conduction band is negligible. At Γ only the antibonding Γ_{15} valence band state interacts with the f states by symmetry and the bonding–antibonding splitting is reduced to 2.5 eV. The large f bandwidth is due in part to this interaction with the oxygen sublattice, as can be verified by calculating the f band without hybridization with the anion sublattice. Because of the sensitivity of the shape of the valence band to the hybridization with the uranium f states it might be possible to determine the strength of this hybridization experimentally by tracing out the top of the valence bands using angle-resolved photoemission. The f-like character in the valence-band region of UO_2 is qualitatively very similar to that found for ThO_2 in fig. 2 because it is largely determined by symmetry. Because the f levels lie closer in energy to the valence bands, however, the mixing is stronger. It should be possible to see this f mixing, if it occurs, by means of energy-dependent photoemission.

The coarse electronic structure of UO_2 is seen experimentally most clearly by means of photoemission.[2,3,8–12] These studies find a valence bandwidth of *ca.* 6 eV and a fundamental bandgap[12] of *ca.* 5 eV, with the final state f level, as seen in X.p.s. in the lower part of the gap. The calculated bands [fig. 6(a)] are in good qualitative agreement with this picture. If we are interested in the finer details of the electronic structure there are, however, many uncertain points. We find, for example, that the valence bandwidth is sensitive to hybridization with the f states and is reduced to 3.7 eV when these are treated as band states [fig. 6(b)]. This is not, however, clearcut evidence for the lack of such strong hybridization. There is a large uncertainty in the measured valence bandwidth arising from low experimental resolution (estimated to be *ca.* 0.4 eV) and unidentified structure at the bottom of the valence band. In addition, a large amount of detailed structure in the calculated density of states (fig. 2) is not reproduced by X.p.s. In principle many of these questions could be resolved by a calculation of the dielectric function which could then be compared with that determined experimentally from reflectivity measurements[7] and the various transitions identified. While such calculations are possible, within a single-particle framework, it is not clear whether the large effort required is at present justified.

ThO_2, UO_2 and PuO_2

We compare the calculated band structures along the Γ–X direction for ThO_2, UO_2 and PuO_2 in fig. 7. The calculations were performed at the experimental lattice constants. For simplicity the f states were omitted from the calculation and the position of the $5f$ orbital energy is indicated by a horizontal line. Inclusion of the f states as band states

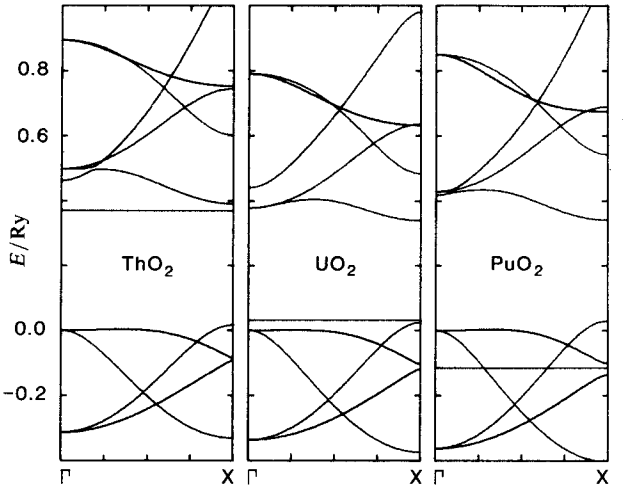

Fig. 7. Energy-band structures of ThO_2, UO_2 and PuO_2 at the experimental lattice constants along the Γ–X direction. The *f* electrons were treated as atomic states and only the 5*f* orbital energy is indicated as a horizontal straight line.

would lead, in a first approximation, to the formation of a band about this orbital energy. The most striking trend along the actinide series is the drop of this *f* level across the gap on going from thorium to plutonium. In the case of ThO_2 the *f* band overlaps the bottom of the conduction band formed by the uranium *d* states, in UO_2 the strong hybridization with the *p* states leads to a gap between the two groups of bands as seen in fig. 6 and in PuO_2 the plutonium *f* states overlap the valence bands. Although, as we have seen, the *f* levels cannot be treated as band states, the position of the *f* resonance agrees with experiment where it has been determined.[12,14,15] The second most notable feature in fig. 7 is the increase in the valence bandwidth going across the series. For ThO_2, UO_2 and PuO_2, respectively, the bandwidths at Γ are 4.3, 4.6 and 5.0 eV and at X, 4.8, 5.4 and 5.9 eV. This increase in bandwidth comes from the decrease in volume, as can be confirmed from a calculation of the volume dependence of the valence bandwidth of a single substance. The valence-band maxima and minima are in all three cases at X. The conduction-band minimum is also always at X. The lowest conduction band state at Γ is the singly degenerate Γ_1 state for ThO_2 and PuO_2, but for UO_2 the Γ_{12} state is lowest.

Pressure Dependence of Electronic Structure of UO_2

Although the 5*f* electrons are not itinerant in UO_2, we have seen above that the position of the 5*f* orbital energy in the self-consistently calculated potential not only describes the trend across the An series correctly but also appears to give the absolute position of the localized *f* states in the fundamental gap, as seen by X.p.s., quite well. Encouraged by this, we can ask how the position of the 5*f* levels and the position and widths of the conduction and valence bands change under compression. Our interest is to see whether it might be possible to delocalize the *f* electrons by applying sufficient pressure. This might happen[40] either by increasing the 5*f* bandwidth, W_f, sufficiently so that it exceeds the Coulomb correlation energy, U_f, and the 5*f* electrons become delocalized or, more likely, by increasing the width of the conduction band so that it overlaps the localized 5*f* states and becomes populated. Although the band gap in LD calculations is often considerably smaller than the experimental gap, it appears from recent calculations that the metallization volume is given quite well.[41] In fig. 8 we plot the energy bands of UO_2

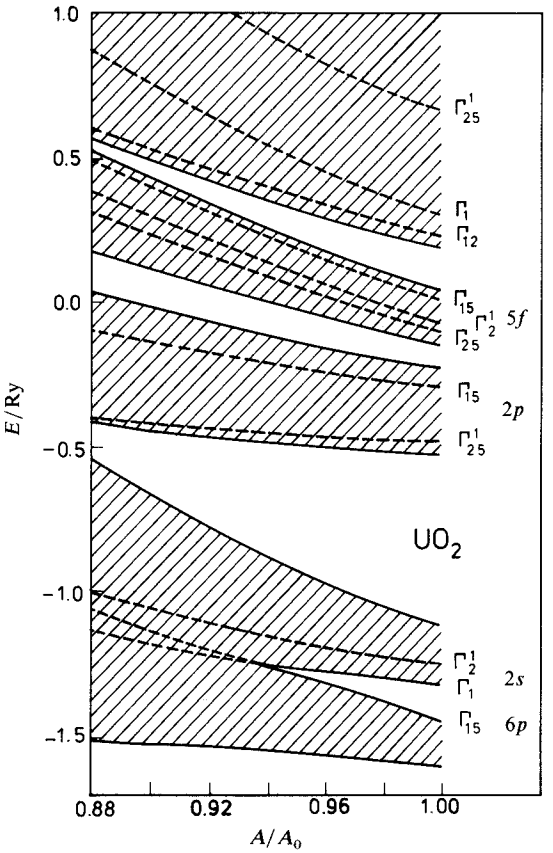

Fig. 8. Energy-band structures of UO_2 as a function of the lattice constant. The f electrons are included as band states. Only the top and bottom of the bands and the bands at the Γ point are shown. The labels on the right-hand side indicate the majority character of the bands.

as a function of lattice parameter down to a volume 30% smaller than the equilibrium volume. For clarity, only the band extremities and some high-symmetry points are shown. With decreasing volume the centres of gravity of the bands rise in energy and the bands broaden. The largest effect is seen in the uranium $6p$ and oxygen $2s$ states. These form a band which, already very wide at the equilibrium volume, broadens very rapidly under pressure. The position of the bonding states changes fairly slowly with pressure, while the antibonding states rise rapidly, giving a large repulsive contribution in the total energy. The neglect of the large spin–orbit splitting for the $6p$ states should not affect the total energy significantly since these states are fully occupied.

Higher in energy we find that the fundamental gap increases under pressure. However, the $5f$ levels rise faster than the bottom of the conduction band, so that eventually a metal–insulator transition should take place when they cross. We cannot, of course, calculate accurately at what volume this should take place, but we can put an upper bound on the transition volume as that volume where the top of the f band crosses the bottom of the conduction band. This volume is obtained by extrapolating the f–d gap in fig. 8 to zero value, as shown in fig 9 (an explicit calculation at smaller volumes would require treating the uranium $6s$ level as a band state). This indicates that it is necessary to reduce the lattice constant to $<82\%$ of the equilibrium value (or 55% of the volume) before a transition might occur. From fig. 7 it would clearly be

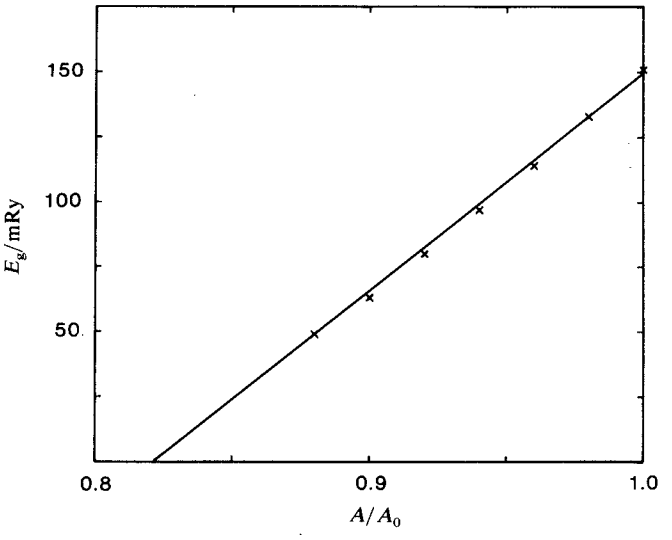

Fig. 9. Gap between the top of the 5*f* band and the conduction band minimum for UO_2 as a function of the lattice constant. The lattice constant at which the gap extrapolates to zero is 82% of the zero-pressure lattice constant.

more promising to try to delocalize the single *f* electron in PaO_2 by this mechanism since we expect the *f* level to lie considerably closer to the conduction band edge and a smaller pressure would be required.

A rough criterion[40] for the 5*f* electrons to undergo a Mott transition is that the 5*f* bandwidth, W_f, must exceed the Coulomb correlation energy, U_f, deduced from photoelectron spectroscopy[12] to be *ca.* 4.5 eV. At the equilibrium lattice constant in fig. 8 W_f is 2.6 eV and increases rapidly with pressure. It becomes larger than U_f at a lattice constant equal to 89% of the equilibrium value (or 71% of the equilibrium volume). Thus to metallize UO_2, this mechanism would appear to be more promising than the level-crossing mechanism considered above, especially as U_f ought to decrease with increasing pressure. There is, however, a large uncertainty in predicting a critical volume for this mechanism because of the qualitative nature of the criterion $W_f > U_f$. Absorption measurements of the intra-5*f* transitions[42] under pressure would be useful to examine changes in the localized *f* states.

Conclusions

In this paper we have extended previous calculations[18,19] of the ground-state properties of UO_2 to ThO_2 and PuO_2. The calculated results for all three compounds agree satisfactorily with the measured values. In particular, the cohesive energy is a much more sensitive measure of the quality of the calculation than the lattice energy. The 5*f* An states, however, may not be treated as simple band states since this then leads to a lattice collapse.

By including the An 6*p* states explicitly as bands we were able to examine the effect of reducing the radius of the An Wigner-Seitz sphere on the electronic charge inside that sphere. A 4+ An ion can only be achieved by excluding 6*s* and 6*p* charge density from the An volume. This casts serious doubt on the validity of treating AnO_2 as fully ionic which is how it is normally modelled.[37-39] Similarly, the large valence bandwidth can be expected to lead to deviations from behaviour predicted by an ionic model in which this width is considered negligible.

The calculated $5f$ bandwidths are comparable to the Coulomb correlation energy, deduced from photoelectron spectroscopy,[12] so that it might be possible to delocalize the f electrons by applying pressure. Calculations at reduced volumes indicate that this is more likely to happen in UO_2 than a band-crossing transition, but both transitions only occur at very high pressures. In PaO_2, on the contrary, a band-crossing transition should occur at much lower pressures.

References

1 A. A. Sviridova and N. V. Suikovskaya, *Opt. Spectrosk.*, 1965, **22**, 940 (*Opt. Spectrosc.*, 1967, **22**, 509).
2 B. W. Veal and D. J. Lam, *Phys. Rev. B*, 1974, **10**, 4902.
3 J. C. Fuggle, A. F. Burr, L. M. Watson, D. J. Fabian and W. Lang, *J. Phys. F*, 1974, **4**, 335.
4 B. C. Frazer, G. Shirane, D. E. Cox and C. E. Olsen, *Phys. Rev. A*, 1965, **140**, 1448.
5 J. Faber Jr and G. H. Lander, *Phys. Rev. B*, 1976, **14**, 1151.
6 R. J. Ackerman, R. J. Thorn and G. H. Winslow, *J. Opt. Soc. Am.*, 1959, **49**, 1107.
7 J. Schoenes, *J. Appl. Phys.*, 1978, **49**, 1463.
8 J. Verbist, J. Riga, J. J. Pireaux and R. Caudano, *J. Electron Spectrosc.*, 1974, **5**, 193.
9 S. Evans, *J. Chem. Soc., Faraday Trans. 2*, 1977, **73**, 1341.
10 L. E. Cox, *J. Electron Spectrosc. Relat. Phenom.*, 1982, **26**, 167.
11 G. Chauvet and R. Baptist, *Solid State Commun.*, 1982, **43**, 793.
12 Y. Baer and J. Schoenes, *Solid State Commun.*, 1980, **33**, 885.
13 J. Schoenes, *Phys. Rep.*, 1980, **63**, 302.
14 B. W. Veal, D. J. Lam, H. Diamond and H. R. Hoekstra, *Phys. Rev. B*, 1977, **15**, 2929.
15 D. Courteix, J. Chayrouse, L. Heintz and R. Baptist, *Solid State Commun.*, 1981, **39**, 209.
16 V. A. Gubanov, A. Rosen and D. E. Ellis, *J. Inorg. Nucl. Chem.*, 1979, **41**, 975; *Solid State Commun.*, 1977, **22**, 219.
17 P. J. Kelly, M. S. S. Brooks and R. Allen, *J. Phys. (Paris)*, 1979, **C4**, 184.
18 P. J. Kelly and M. S. S. Brooks, *J. Phys. C*, 1980, **13**, L939.
19 M. S. S. Brooks and P. J. Kelly, *Solid State Commun.*, 1983, **45**, 689.
20 *Theory of the Inhomogeneous Electron Gas*, ed. S. Lundqvist and N. H. March (Plenum, New York, 1983).
21 P. Hohenberg and W. Kohn, *Phys. Rev. B*, 1964, **136**, 864.
22 W. Kohn and L. J. Sham, *Phys. Rev. A*, 1965, **140**, 1133.
23 C. O. Almbladh and U. von Barth, *Phys. Rev. B*, 1985, **31**, 3231.
24 U. von Barth, in *NATO Advanced Study Institute on the Electronic Structure of Complex Systems*, ed. W. Temmerman and P. Phariseau (Plenum, New York, 1984).
25 See *e.g.* A. R. Williams and U. von Barth, in ref. (20).
26 M. S. Hybertsen and S. G. Louie, *Phys. Rev. Lett.*, 1985, **55**, 1418.
27 O. K. Andersen, *Phys. Rev. B*, 1975, **23**, 3060.
28 O. K. Andersen, O. Jepsen and D. Glötzel, in *Proc. Enrico Fermi Int. School of Physics, Course LXXXIX*, ed. F. Bassani, F. Fumi and M. P. Tosi (North-Holland, Amsterdam, 1985).
29 D. Glötzel, B. Segall and O. K. Andersen, *Solid State Commun.*, 1980, **36**, 403.
30 G. B. Bachelet and N. E. Christensen, *Phys. Rev. B*, 1985, **31**, 879.
31 M. S. S. Brooks, B. Johansson and H. L. Skriver, in *Handbook of the Physics and Chemistry of the Actinides*, ed. A. J. Freeman and G. H. Lander (Elsevier, Amsterdam, 1984), chap. 3, pp. 153–269.
32 D. D. Koelling and B. N. Harmon, *J. Phys. C*, 1977, **10**, 3107.
33 We use the frozen core scheme described by O. Gunnarsson, J. Harris and R. O. Jones, *Phys. Rev. B*, 1977, **15**, 3027.
34 D. G. Pettifor, *Commun. Phys.*, 1976, **1**, 141.
35 L. R. Morss, *J. Less Common Met.*, 1983, **93**, 301.
36 K. P. Huber, in *American Institute of Physics Handbook* (McGraw-Hill, New York, 1972), sect. 7g.
37 C. R. A. Catlow, *J. Chem. Soc., Faraday Trans 2*, 1978, **74**, 1901.
38 G. C. Benson, P. I. Freeman and E. Dempsey, *J. Am. Ceram. Soc.*, 1963, **46**, 43.
39 R. A. Jackson, A. D. Murray, J. H. Harding and C. R. A. Catlow, *Philos. Mag. Sect. A*, 1986, **53**, 27.
40 N. F. Mott, *Metal-Insulator Transitions* (Taylor and Francis, London, 1974).
41 S. H. Wei and H. Krakauer, *Phys. Rev. Lett.*, 1985, **55**, 1200.
42 J. Schoenes, *J. Magn. Magn. Mater.*, 1978, **9**, 57.

Paper 7/042; *Received* 7*th January*, 1987